Critical points for predicting 3D printable filaments behaviour

Vicente Linares, Eduardo Galdón, Marta Casas [*], Isidoro Caraballo

Department of Pharmacy and Pharmaceutical Technology, Faculty of Pharmacy, Universidad de Sevilla, C/Profesor García González 2, 41012, Seville, Spain

ABSTRACT

Fractal dimension has been employed for the first time to provide key information about the behaviour of extruded filaments. High drug loaded filaments made of thermoplastic polyurethane and anhydrous theophylline (10–70% w/w of drug content) have been obtained by using a single screw extruder. Fractal analysis was carried out based on the measures of the perimeter of the filaments at different magnification levels, using the box-counting technique approach. The fractal dimension values showed a critical point at 37.8% w/w of drug, which agrees with the behaviour of the printability of the filaments by FDM. The drug percolation threshold derived from drug release results was also in agreement with this critical point. Thus, both approaches concur in the estimation of a critical point around 38% w/w of drug, where printability and dissolution behaviour dramatically change. Therefore, the Fractal Dimension analysis could be considered as a non-destructive, non-expensive and fast method for estimating a crucial parameter for FDM 3D printing as is printability of the filament.

1. Introduction

One of the most recent technologies which has being applied to the pharmaceutical field is the three-dimensional (3D) printing, becoming an opportunity to create a new platform to develop new delivery systems [1,2]. The main 3D printing techniques in the manufacture of pharmaceutical dosage forms are pressure-assisted microsyringe, fused deposition modeling (FDM), inkjet-based systems, stereolithography and selective laser sintering. All techniques are based on a layer by layer approach to build complex and tailored designs, but the principle of operation varies greatly from one technology to another [3]. Among them, Fused Deposition Modeling (FDM) is widely used because of its versatility, ease of use, low cost and compact size equipment [4]. This technology works with thermoplastic filaments fabricated by hot melt extrusion technique or filament extruders. In both cases, the process requires high temperature and a blend with specific requirements, especially from the rheological point of view. Therefore, the development of drug loaded filaments adequate for FDM processing involves higher complexity due to the usually poor rheological properties of the APIs. Several thermoplastic polymers have been reported to show adequate printing properties (hardness, melt flow rate, tensile strenght, rigidity, etc.) to manufacture medicines, including polyvinylalcohol, acrylic derivatives, polyurethanes, etc. [5–7]. Depending on the melting point of the drug, this component can be melted or not in the blend

during the extrusion process. This fact will exert a great influence on the properties of the filament. Although some studies have evaluated the effect of the rheological, thermal, and mechanical characteristics of filaments on their printability [8], a deep knowledge of the factors governing the filament properties is still necessary. The roughness is a characteristic that has not been studied thoroughly in 3D printing until now. We believe roughness analysis can provide valuable information regarding filament characterization. The description of rough surfaces and irregular shapes involves a complex analysis since they cannot be completely described by the conventional Euclidean geometry. The fractal approach, based on self-similarity concept, provides very interesting tools able to express the irregularities of a perimeter, a surface or a volume through very simple parameters, the fractal dimensions.

Regarding the field of Pharmaceutical Technology, fractal-like structures have been observed in the distribution of drugs and excipients. This has allowed to obtain additional information about critical properties of the dosage forms, like hardness or kinetic behaviour of tablets [9]. Thus, fractal dimensions have been employed to improve the understanding of physical and technological properties of pharmaceutical systems like powders, gels, emulsions, tablets or nanoparticles [9–12].

Geometric aspects are crucial in order to gain knowledge and to better understand the behaviour of dosage forms and pharmaceutical systems [12]. However, fractal dimension has not yet been applied to

---

filaments considered as drug delivery systems or as suitable materials for FDM 3D printing of dosage forms. Fractal analysis is expected to contribute to the knowledge based on mechanistic considerations related to the morphological and/or topological characteristics of these extruded filaments.

Regulatory agencies are promoting the application of physical or mathematical models based on scientific knowledge with the objective of improving the quality of pharmaceutical products from the design step. In this context, percolation theory is a physical model that has demonstrated to be useful in the comprehension of pharmaceutical systems where approaches based on continuous models fail to explain their behaviours [13,14]. Drug loaded filaments can be described as systems in which drug and polymeric excipient are randomly distributed in a network. The study of these blends, which behave as non-continuous systems, can be carried out thanks to percolation theory. The application of this model allows to analyse properties or predict behaviours near to the percolation thresholds of these systems. These thresholds represent geometrical phase transitions, in which a component starts to percolate the system. That means that the particles of this component constitute a cluster of neighbor positions spanning the whole system. When a component reaches its percolation threshold, its influence on the properties of the system increases. Thus, close to the percolation thresholds, significant changes of the system properties can occur, generating the so-called critical points. Critical points related to properties as relevant as drug release, mechanical characteristics, rheological properties or water uptake, among others have been found in pharmaceutical systems [9,12–30].

In this work, a mathematical approach as the fractal analysis and a complementary physical model as percolation theory, will be applied for the first time to study the behaviour of extruded filaments. The existence of critical points will be investigated on two different properties of the strands. The first one involving the printability behaviour that makes filaments suitable feedstock material to be printed by FDM. The second one related to the drug release behaviour of filaments. As it is well known, these points constitute natural limits of the Design Space of a pharmaceutical formulation [31]. Therefore, the knowledge of the critical points will facilitate the application of the Quality by Design approach in future developments.

According to the above, the objective of this work is the use of fractal analysis to study the behaviour of drug loaded filaments extruded by a single-srew extruder. For this aim, filaments made of binary mixtures of thermoplastic polyurethane and theophylline as model drug will be analysed to estimate critical points associated to key properties as drug release and mechanical behaviour. These points are related to geometrical phase transitions of the components in the system, thus, they could make possible the prediction of some important properties as the printability.

2. Materials and methods

2.1. Materials

Anhydrous theophylline (batch151209-P-1, Acofarma, Barcelona, Spain) was used as model drug. Medical grade thermoplastic polyurethane Tecoflex™ EG-72D (TPU) was used as matrix forming excipient, which was supplied by Lubrizol Advanced Materials (Barcelona, Spain).

2.2. Methods

2.2.1. Preparation of drug-loaded filaments

Pellets of TPU were frozen using liquid nitrogen to mill them (Retsch ZM 200, Haan, Germany) using a 1.0 mm output sieve (mean diameter 227.9 ± 166.0 μm). A drug particle size lower than 180 μm (mean diameter 121.5 ± 45.0 μm) was used. Binary mixtures of drug and polymer powder (10–70% w/w proportion) have been mixed during 15

min (Turbula mixer, Willy A. Bachofen, Basel, Switzerland). The optimum blend time was determined according to a previously published method [11].

The blends were extruded using a single screw extruder Noztek Pro (Noztek, Sussex, UK) at an extrusion temperature of 130 °C for all mixtures. Screw speed selected was 15 rpm and the nozzle diameter was 1.75 mm. Drug loaded filaments were then stored at 25 °C before the printing process.

2.2.2. Thermal analysis of filaments

Filaments were analysed by differential scanning calorimetry (DSC) (Setaram-DSC 131, Caluire, France). About 5 mg of sample was hermetically sealed in an aluminum pan and heated from 30 to 300 °C at a rate of 5 °C/min.

2.2.3. Physical characterization of filaments

Considering that FDM feedstock material should have a diameter value of 1.75 mm, as indispensable requirement for 3D printing, filaments obtained were measured using a digital micrometer (VWR International, Leuven, Belgium).

2.2.4. 3D printing process

3D printed systems were manufactured with a Raise3D Pro2 printer (Raise3D Technologies, Inc, California, USA). The software BlocksCAD (BlocksCAD Inc., Massachusetts, USA) was used to design the 3D printed systems. The printing settings were as follows: nozzle diameter of 0.4 mm, layer thickness 0.3 mm, nozzle temperature 190 °C, heated bed temperature 70 °C and the printing speed 80 mm/s, to produce systems with height of 5 mm and diameter of 10 mm.

2.2.5. Scanning electron microscopy (SEM)

The surface of the filaments was evaluated using scanning electron microscopy (SEM) with a FEI TENEO electronic microscope (FEI Company, Hillsboro, OR, USA), operating at 5 kV. Filamnets were coated with a 12 nm thin Pt/Pd layer with Leica EM SCD500 high vacuum sputter coater.

2.2.6. Fractal analysis. Box-counting technique

The box-counting technique is based on the analysis of perimeter from binary images, considering every pixel as a "box". Through this technique we can calculate the fractal dimension value following the next equation [32] (1):

$$N(\lambda) = C\lambda^{-D} \tag{1}$$

Where N is the number of boxes, C is a constant of proportionality, λ is the box side length and D is the fractal dimension.

In this case, the roughness of the filaments was studied by taking photographs with a stereo microscope SMZ800N (Nikon Instruments Inc., New York, USA). Images of each filament containing different drug content were taken with different zoom ratio (1x to 8x). Pixel modification was carried out thanks to the Nikon software (Nis-Elements BR 5.20.02) by increasing the pixel size ten times more than the original one (800x and 80x). This software was also used to binarize each photography. The perimeter measured in pixels was obtained with Matlab R2019b (The MathWorks, Inc., Massachusetts, USA). Pixels were converted into centimeters (cm) thanks to the Nikon software conversion pixel/cm. Sixteen images were studied for each filament from 10 to 70% of drug content, entailing a total of 112 images analysed.

2.2.7. Dissolution testing and modeling

The dissolution studies were carried out using a USP Apparatus II (Sotax AT7 smart, Allschwil, Switzerland) with a rotation speed of 50 rpm, in 900 ml of distilled water at 37 ± 0.5 °C. About 100 mg of filament for each lot and printed systems were analysed by triplicate. Filtered samples were withdrawn at specific interval times (15, 30, 60,

90, 120, 180, 240, 300, 360, 420, 480, 1440 min). The percentage of drug released was measured in a UV–Vis spectrophotometer Agilent 8453 (Agilent Technologies, California, CA, USA) at 272 nm. Sink conditions were guaranteed during the whole study.

Drug release data ($M_t/M_\infty \leq 0.6$) were analysed according to zero order, Higuchi (1963) [33], Korsmeyer et al. (1983) [34] and Peppas and Sahlin (1989) [35] equations (2)–(4):

$$\frac{M_t}{M_\infty} = bt^{1/2} \tag{2}$$

$$\frac{M_t}{M_\infty} = k^k t^n \tag{3}$$

$$\frac{M_t}{M_\infty} = k_d t^m + k_r t^{2m} \tag{4}$$

where M_t/M_∞ is the drug released fraction at time t (the drug loading was considered as M_t), b and k^k are kinetic constants characteristic of the drug/polymer system, t is the release time, n is the release exponent that depends on the release mechanism and the shape of the matrix tested [35], k_d and k_r are the diffusion and relaxation rate constants, respectively, m is the purely Fickian diffusion exponent for a device of any geometrical shape which exhibits controlled release. Determination coefficient (r^2) was used to test the applicability of the release models.

2.2.8. Estimation of percolation thresholds

In order to estimate the percolation thresholds, results from fractal analysis and dissolution study parameters were analysed to observe possible discontinuities related to geometrical phase transitions of components.

According to Bonny and Leuenberger [36] the percolation thresholds related to drug release behaviour can be determined by means of the system property β (Eq. (5)):

$$\beta = \frac{b}{\sqrt{2A - \varepsilon C_s}} \tag{5}$$

where b is the Higuchi's slope from a plot of the cumulative amount Q of drug released per unit surface area versus the square root of the time t, C_s is the solubility of the drug in the permeating fluid, ε is the total porosity of the system, i.e., the pores and drug, and A is the concentration of the dispersed drug in the system.

According to Higuchi's equation, the surface area between drug and medium, where the release takes place, should be taken into account except in the case that it is constant [37]. In our systems, this surface area is decreasing with time. To address this issue, Fessi et al. [38] proposed the following equation (Eq. (6)) to calculate the diffusional cross section of a cylinder:

$$o_t = \frac{2\pi}{t} \int_0^t \left\{ \left(r_0 - \frac{k}{2}t \right)^2 + \left(r_0 - \frac{k}{2}t \right)(h_0 - kt) \right\} dt \quad t > 0 \tag{6}$$

where O(t) is the diffusional cross section and k is a rate constant which shows the linear dependence with time of radius (r) and height (h) of the region containing solid drug.

Our research group has adapted this method to calculate the values of diffusional cross section in filaments [37]. Assuming the homogeneous distribution of the drug in the system, the exposed area can be proportionally calculated with the decrease of drug in function of time. So, when calculating b, the theophylline released at each time was divided by this area exposed by the drug, to transform the amount of drug released (mg) in amount of drug released per surface area (mg/cm^2).

Finally, the values of β for filaments with theophylline loadings from 20% to 70% (w/w) versus total porosity (after leaching) will be evaluated for the estimation of drug and excipient percolation thresholds.

Regarding the total porosity, it was calculated with following equation (7):

$$\varepsilon = \frac{Vs - Ve}{Vs} \tag{7}$$

where V_s is the volume of the filament and V_e is the volume occupied by the excipient.

3. Results and discussion

Binary blends of theophylline and thermoplastic polyurethane (10–70% w/w of drug) were extruded at 130 °C employing a single-screw extruder. According to the printing process, filament diameters from 1.75 ± 0.1 mm can be accepted since they allow the drive wheels to print with accuracy. All drug-loaded filaments showed suitable diameter to be printed by FDM (1.69–1.82 mm) with the exception of filaments with 30 and 40% w/w, with slightly smaller diameter than the lower limit (1.56–1.64 mm).

Regarding the thermal analysis, results from differential scanning calorimetry of pure components confirmed the stability and compatibility of these materials (Supplementary data, Fig. S1).

The morphology of the loaded filaments was analysed by SEM (Fig. 1). According to the characteristics of components, filaments are suspension-type solid dispersion with theophylline particles dispersed in the continuous medium formed by TPU. The microphotographs of the filaments reveal the roughness and the porosity change with the increasing amount of drug. The thermoplastic excipient gets to create a continuum medium, surrounding the drug particles in a very effective way (Fig. 1h). Since crystals of theophylline are soaked in the continuous polymer matrix [29], the continuum percolation model is expected to describe the systems obtained. This model considers a continuum distribution of the components, in which the percolation threshold of a substance can be found at approximately 16% v/v of its occupation probability or volume concentration [29,39]. According to that, in all the batches the excipient is above its percolation threshold, thereby resulting in a coherent matrix which controls the drug release.

Morphological analysis of the extruded filaments was carried out based on the fractal analysis. The box-counting technique was applied to analyse the filaments' roughness from perimeter images [32]. To make this possible, 16 images from 3 different filaments for each batch (10–70% of drug content) were taken by the stereo microscope, giving a total of 112 images. These images were binarized to reduce the information available in the photograph, thus facilitating the analysis of interesting areas. In this process, the image is reduced to true-false information, which can be understood as values of 1 or 0, represented as black and white images (Fig. 2). The analysis was carried out using Matlab, which can detect the perimeter of the filament, providing the number of pixels (boxes) that make up that perimeter. The photograph of the perimeter only includes one side of the filament to make it easier for Matlab the detection of the perimeter and its analysis. Once the perimeter was converted to cm, this value was represented versus the inverse of the zoom ratio (1/1 to 1/8) (Fig. 3). As a result, the fractal dimension value was obtained from the corresponding exponent of each equation (Table 1).

The increase of solid particles in the system will make it more difficult to displace the blend through the extruder and will result in a change in the extruded filament. The application of percolation theory in the morphological study can help to the identification of the point in which the quantity of drug exerts more influence on the system, i.e., percolates. Based on this idea, roughness results were analysed according to percolation theory to investigate the existence of critical points. Following this approach, fractal dimension was plotted versus the drug percentage to observe possible discontinuities (Fig. 4). It is expected that a higher percentage of drug implies a higher roughness, and therefore, a higher fractal dimension. However, Fig. 4 shows that
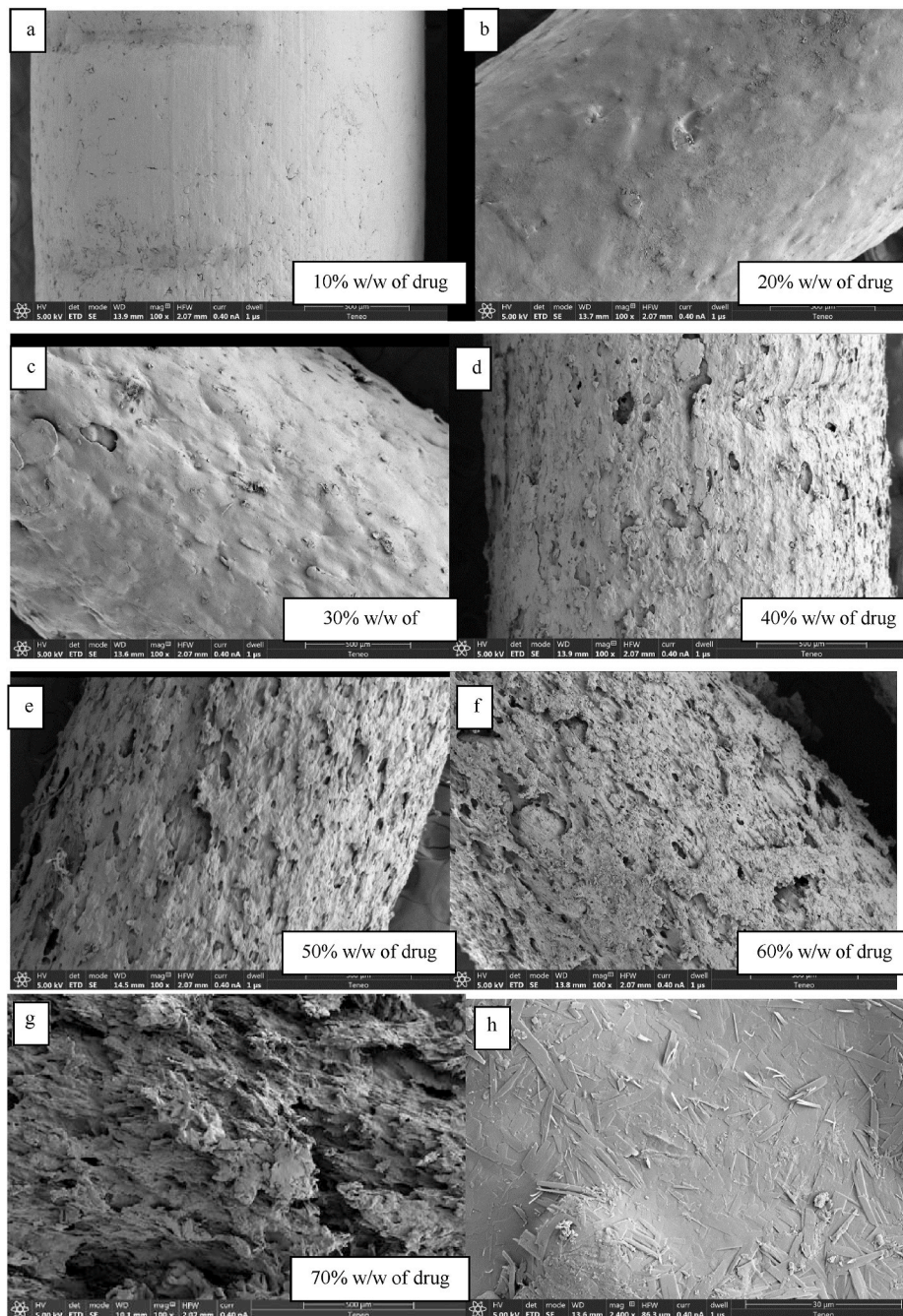
Fig. 1. Microphotographs of filaments composed by theophylline-thermoplastic polyurethane from 10 to 70% w/w of drug (a–g), and detail of filament surface with 30% w/w of drug (h).

this premise did not meet for filaments with 10–20% w/w of drug. A possible explanation is that those strands with a high percentage of melted TPU (80–90% w/w) were more malleable than those with less excipient content. Due to the throbbing extrusion because of the movement of the single screw, filaments with 80% w/w and 90% w/w of polymer reflected in their perimeter the pulsating extrusion. This increased the on dulations and irregularities on the surface of the filament, resulting in a higher fractal dimension. Nevertheless, a 30% w/w of drug content was enough to contribute to the rigidity of the filament, thus, making it less sensitive to the pressure variability during the extrusion. Fig. 4 shows a change of trend between the 30% w/w and 40% w/w of theophylline. Since drug loaded filaments can be described as binary systems where drug and polymer are randomly distributed in a network, two percolation thresholds can be found. The discontinuity

observed at 30–40% w/w of drug can be associated to a possible geometric phase transition of the drug, so-called critical point [14]. The Fuertes' method, based in the Effective Medium Approximation [40,41], allows the use of linear regressions above and below the threshold in order to estimate the critical point as the intersection between both regression lines (Fig. 4). The good determination coefficient of the linear regression for both trends (10–30% w/w and 40–70% w/w), with a R^2 higher than 0.9, illustrates the adequate fit of the experimental data with the theory and methodology applied. The critical points estimated using the Fuertes' method was 29.69% v/v (37.8% w/w) of drug. Below this critical point the filaments will have clusters of theophylline particles encapsulated by the excipient, so-called finite clusters, resulting in less influence on the system. Above this critical point, the drug will be found as clusters of neighbouring occupied sites extended from one side to the
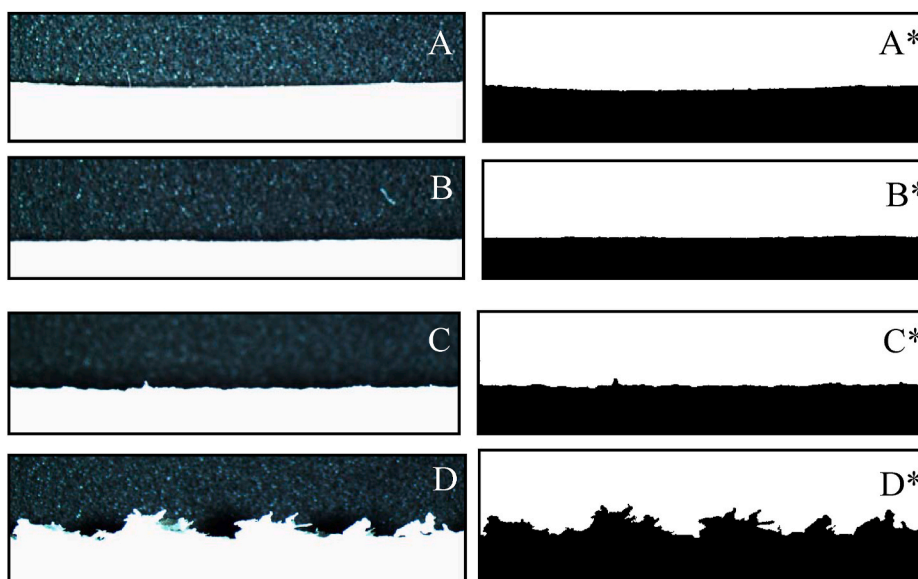
Fig. 2. Images of filaments taken by stereo microscope SMZ800N (A–D) and binarized images corresponding to the original ones (A*-D*). Filament with 10% of drug (A-A*), filament with 30% of drug (B–B*), filament with 40% of drug (C–C*) and filament with 70% of drug (D-D*).
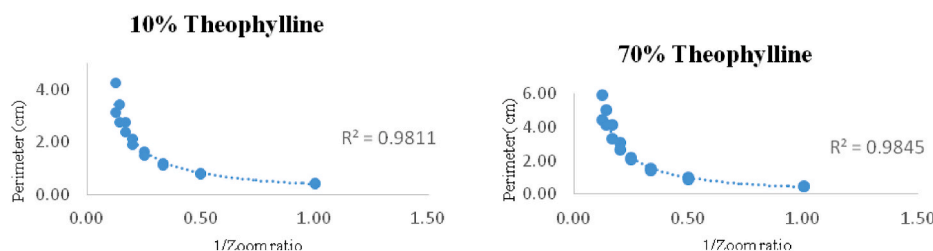

Fig. 3. Graphical representation of the perimeter and the inverse of the zoom ratio for 10% and 70% of drug loaded filament.

Table 1
Fractal dimension values defined by the equation of the graph from different drug contents.

Drug content (%)	Regression Equation	Fractal dimension
10	$y = 0.4121x^{-1.017}$	1.017
20	$y = 0.4164^{-1.01}$	1.010
30	$y = 0.4205^{-1.001}$	1.001
40	$y = 0.4214^{-1.013}$	1.013
50	$y = 0.4624^{-1.057}$	1.057
60	$y = 0.4572^{-1.081}$	1.081
70	$y = 0.4375^{-1.174}$	1.174

Fig. 4. Graphical representation of the fractal dimension versus drug percentage of each filament.

rest of the sides of the matrix, which is so-called infinite cluster or percolating cluster. Therefore, above its critical point the drug increases its influence on the filament, resulting, for example, in important changes on the printability of the filaments, making them more rigid and less plastic.

Taking into consideration that filaments were extruded through a single-screw extruder, these estimations fully agree with the results obtained when the filaments are employed to feed the 3D printer: only filaments up to 30% w/w of drug, i.e., below the critical point of the drug, were successfully printed, according to the previously performed digital design (see Fig. 5). On the other hand, the filaments above the critical point of the drug (40–70% w/w of theophylline), failed to be printed. Thus, it could be reasonable to believe that the roughness of the filament is directly connected with its printability. This statement can be applied to mixtures of thermoplastic polymers that melt in the process and drugs with a high melting point, that remain as crystalline particles.
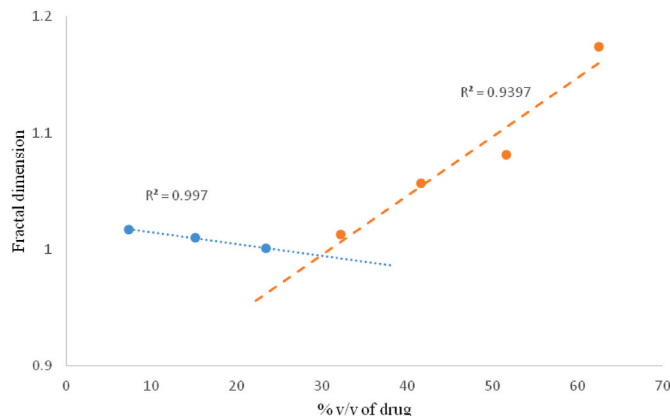
Therefore, fractal analysis could be useful to predict the printability of this kind of filaments, without need of using more expensive and/or destructive methods. However, further studies are needed to verify this hypothesys with powder mixtures.

Drug release profiles from filaments and 3D printed systems are shown in Fig. 6. As expected, higher drug release rates were found as the drug concentration increases. Regarding filaments, the minimum percentage of drug released from batches with lower drug content suggests a release only from particles in contact with the filament surface.

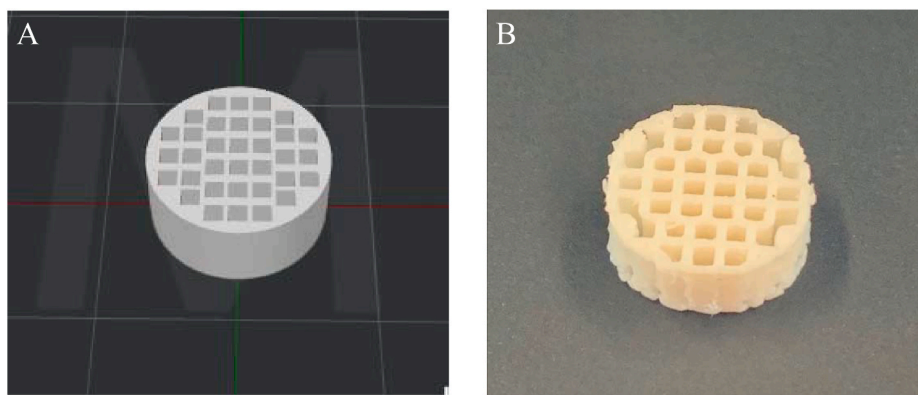With respect to the 3D printed systems, the drug release rates were

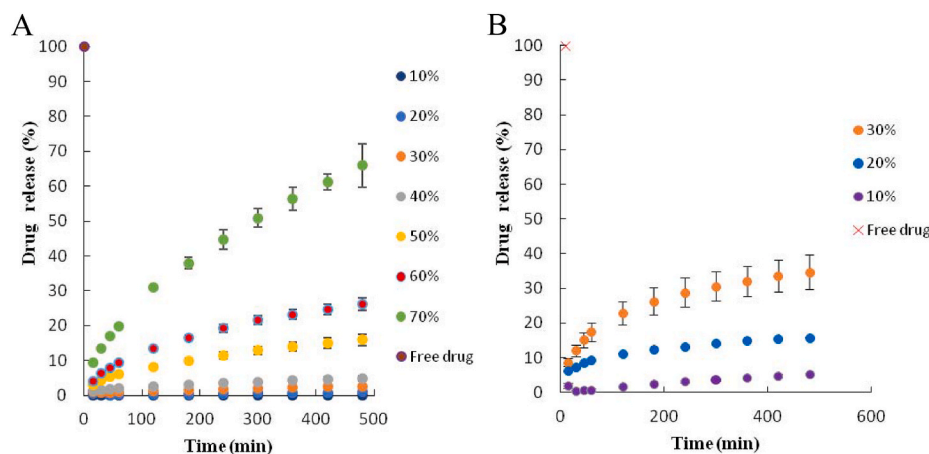**Fig. 5.** A) Digital design of the 3D printed system. B) 3D printed system with a 30% of drug content.

Fig. 6. Drug release profiles from filaments (10–70% w/w of drug) (A) and 3D printed systems (10–30% w/w of drug) (B).

up to 30 times higher compared to the filaments with the same drug content. From our point of view, the processing temperature difference between the filament and the 3D printed system is not playing a main role. This significant difference in the drug release rate can be explained better by the increase of the total surface area and surface area to volume ratio for 3D printed systems.

Dissolution data have been analysed according to the different kinetic equations of section 2.2.8 (Tables 2–3). Filaments with 10% w/w of drug were not analysed due to the minimal drug released. The good determination coefficients of drug release profiles for the Higuchi's model reveal a diffusion mechanism for the filaments, except in the case of 20% w/w. Korsmeyer n values close to 0.5 and the predominance of k_d values from Peppas and Sahlin model confirm the diffusional mechanism for these batches, which is typical for inert matrix systems. In the case of batch of 20% w/w, the different drug release mechanism can be the result of the limited access of the solvent to the drug particles.

With respect to the kinetic results from 3D printed systems, these dosage forms show higher values for Higuchi kinetic constant than filaments with the same proportion, as previously observed in drug release profiles. Batches with 20–30% w/w of drug show diffusion mechanism, according to Korsmeyer n values and the predominance of k_d respect to k_r. In the case of the system with the lowest drug percentage, the release kinetics can again be masked by the little fraction of drug that has been released, as occurred with filaments.

Dissolution results were also analysed from the percolation theory point of view. As described in section 2.2.8, the values of the β parameter were calculated considering the different surface area exposed for the drug to the dissolution medium at each time point, in order to fulfil the assumption of Higuchi's equation [37]. These surface areas were estimated based on the parameter $O_{(t)}$ proposed by Fessi et al. [38] and adapted by our research group [37]. The results are shown in Table 2. Fig. 7 shows a plot of β versus the total porosity of the filaments.

Table 2
Main kinetic parameters, total porosity and property β of filaments.

Batches (% w/w of drug)	Zero order	Higuchi		Korsmeyer		Peppas and Sahlin			Total porosity	β (g$^{1/2}$ cm$^{-1/2}$ min$^{-1/2}$)
	r^2	b	r^2	n	r^2	K$_d$	K$_r$	r^2		
20	0.7141	0.0005	0.6322	0.914	0.3948	0.0007	0.00005	0.7587	0.2684	2.916
30	0.9741	0.0011	0.9764	0.3677	0.908	0.0006	0.00002	0.9828	0.2953	9.665
40	0.9850	0.0020	0.9959	0.3902	0.9818	0.0014	0.00003	0.9991	0.3705	21.895
50	0.9658	0.0072	0.9997	0.4794	0.9997	0.0076	−0.00002	0.9998	0.4350	82.064
60	0.9557	0.0123	0.9985	0.5275	0.9981	0.0148	−0.0001	0.9997	0.4979	158.803
70	0.9755	0.0317	0.9993	0.5700	0.9995	0.0282	0.0001	0.9997	0.6792	1029.294

b, Higuchi kinetic constant; n, release exponent; k$_d$, Peppas diffusion kinetic constant; k$_r$, Peppas relaxation kinetic constant; r^2, determination coefficient.

Table 3
Main kinetic parameters of 3D printed systems.

Batch (% w/w of drug)	Zero order	Higuchi		Korsmeyer		Peppas and Sahlin		
	r^2	b	r^2	n	r^2	K_d	K_r	r^2
10	0.9302	0.0025	0.8813	0.9469	0.9928	0.0021	0.00003	0.9991
20	0.9135	0.0053	0.9834	0.2729	0.9969	0.0088	0.0001	0.9969
30	0.8926	0.0142	0.9747	0.3934	0.9865	0.0269	−0.0005	0.9991

b, Higuchi kinetic constant; n, release exponent; k_d, Peppas diffusion kinetic constant; k_r, Peppas relaxation kinetic constant; r^2, determination coefficient.
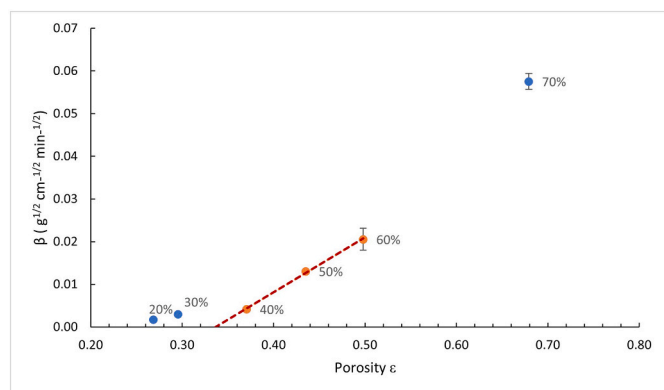
Fig. 7. Tablet property β versus the total porosity ε of drug loaded filaments.

According to the method of Bonny and Leuenberger, the interception with the X-axis of the regression line of the β-values showing a linear trend above the threshold (in our case, the filaments containing from 40 to 60% w/w of drug) gives an estimation of the drug percolation threshold. The obtained result is 0.35 v/v total porosity, which corresponds to a drug percolation threshold of 30.69% v/v of drug content.

This result agrees with drug percolation thresholds obtained for inert matrices (25–35% v/v) [31]. The value of this threshold depends on the three dimensional lattice type (diamond lattice, simple cubic or body-centered cubic lattice) [42]. According to our percolation threshold, it follows that the geometrical distribution of the particles of theophylline and TPU corresponds to the simple cubic lattice.

Below 30.69% v/v of drug content, an incomplete drug release can be expected due to the fact that some of the finite clusters of drug particles do not have access to the dissolution medium. On the other hand, above this critical point, the drug will exert more influence on the filament, resulting in a change on the drug release behaviour.

The critical point associated to drug percolation threshold (30.69% v/v) is very close to the value obtained by fractal dimension (29.69% v/v). So, the geometrical phase transition of the drug in the filaments can be confirmed around 37.8–38.1% w/w. The almost exact agreement between the critical points estimated from the two approaches suggests the important role that the fractal analysis can play in the estimation of the behaviour of the filaments for 3D printing.

4. Conclusions

High drug loaded filaments based on a thermoplastic polyurethane excipient and theophylline as model drug have been successfully obtained using a single screw extruder. These pharmaceutical filaments have been analysed for the first time based on Fractal geometry, concluding that the linear Fractal Dimension obtained from measures of the perimeter of the filaments at different magnification levels, allows to estimate a critical point directly related with a key parameter as is the printability of the filaments by FDM. In addition, the percolation threshold of the drug loaded in the filaments has been estimated for the first time using the method of Bonny and Leuenberger and adapting equation O(t), which estimates the surface exposed by the drug at any time point. We also can conclude that the drug percolation threshold and its associated critical point, both derived from the release behaviour of the filaments, show an almost perfect agreement with the previously obtained from visual observation of the roughness of the filaments, based on Fractal Dimension, which in turn has been found to be related with the printability. So that the agreement between the two approaches (geometrical-mechanical approach based on Fractal Dimension *versus* release behaviour based on percolation theory) support the use of the first one as a non-destructive, non-expensive and fast method for estimating the geometrical phase transitions of the components of the filament that affect its mechanical behaviour, including a crucial parameter for FDM 3D printing as is printability of the filament.

Furthermore, the application of both approaches provides relevant information for a science-based development of the pharmaceutical formulations, allowing an accurate estimation of the Design Space, according to the PAT initiative and the subsequent ICH Q8 guideline.

Author contributions

V.L., Conceptualization, Methodology, Writing - original draft; E.G., Methodology and review; M.C., Conceptualization, Writing - original draft; I.C., Conceptualization, Supervision, Writing - review & editing.

Declaration of competing interest

None.

Acknowledgements

Appendix A. Supplementary data

Supplementary data to this article can be found online at https://doi.org/10.1016/j.jddst.2021.102933.

References

[1] V. Linares, M. Casas, I. Caraballo, Printfills, 3D printed systems combining fused deposition modeling and injection volume filling. Application to colon-specific drug delivery, Eur. J. Pharm. Biopharm. 134 (2019), https://doi.org/10.1016/j.ejpb.2018.11.021.

[2] Á. Aguilar-De-leyva, V. Linares, M. Casas, I. Caraballo, 3D printed drug delivery systems based on natural products, Pharmaceutics 12 (2020) 1–20, https://doi.org/10.3390/pharmaceutics12070620.

[3] I.J. Solomon, P. Sevvel, J. Gunasekaran, A review on the various processing parameters in FDM, Mater. Today Proc. (2020) 10–15, https://doi.org/10.1016/j.matpr.2020.05.484.

[4] P. Khatri, M.K. Shah, N. Vora, Formulation strategies for solid oral dosage form using 3D printing technology: a mini-review, J. Drug Deliv. Sci. Technol. 46 (2018) 148–155, https://doi.org/10.1016/j.jddst.2018.05.009.

[5] G. Verstraete, A. Samaro, W. Grymonpré, V. Vanhoorne, B. Van Snick, M.N. Boone, T. Hellemans, L. Van Hoorebeke, J.P. Remon, C. Vervaet, 3D printing of high drug loaded dosage forms using thermoplastic polyurethanes, Int. J. Pharm. 536 (2018) 318–325, https://doi.org/10.1016/j.ijpharm.2017.12.002.

[6] K. Pietrzak, A. Isreb, M.A. Alhnan, A flexible-dose dispenser for immediate and extended release 3D printed tablets, Eur. J. Pharm. Biopharm. Off. J. Arbeitsgemeinschaft Für Pharm. Verfahrenstechnik e.V. 96 (2015) 380–387, https://doi.org/10.1016/j.ejpb.2015.07.027.

[7] C.I. Gioumouxouzis, A. Baklavaridis, O.L. Katsamenis, C.K. Markopoulou, N. Bouropoulos, D. Tzetzis, D.G. Fatouros, A 3D printed bilayer oral solid dosage form combining metformin for prolonged and glimepiride for immediate drug delivery, Eur. J. Pharm. Sci. 120 (2018) 40–52, https://doi.org/10.1016/j.ejps.2018.04.020.

[8] R. Thakkar, R. Thakkar, A. Pillai, E.A. Ashour, M.A. Repka, Systematic screening of pharmaceutical polymers for hot melt extrusion processing: a comprehensive review, Int. J. Pharm. 576 (2020) 118989, https://doi.org/10.1016/j.ijpharm.2019.118989.

[9] N. Pippa, A. Dokoumetzidis, C. Demetzos, Macheras Panos, on the ubiquitous presence of fractals and fractal concepts in pharmaceutical sciences: a review, Int. J. Pharm. 456 (2013) 340–352.

[10] J. Bonny, H. Leuenberger, Determination of fractal dimensions of matrix-type solid dosage forms and their relation with drug dissolution kinetics, Eur. J. Pharm. Biopharm. 39 (1993) 31–37.

[11] E. Galdón, M. Casas, I. Caraballo, Achieving high excipient efficiency with elastic thermoplastic polyurethane by ultrasound assisted direct compression, Pharmaceutics 11 (2019) 157, https://doi.org/10.3390/pharmaceutics11040157.

[12] R. Abreu-Villela, M. Kuentz, I. Caraballo, Benefits of fractal approaches in solid dosage form development, Pharm. Res. (N. Y.) 36 (2019), https://doi.org/10.1007/s11095-019-2685-5.

[13] H. Leuenberger, B.D. Rohera, C. Haas, Percolation theory – a novel approach to solid dosage form design, Int J Pharm 38 (1987) 109–115.

[14] E. Galdón, M. Casas, M. Gayango, I. Caraballo, First study of the evolution of the SeDeM expert system parameters based on percolation theory: monitoring of their critical behavior, Eur. J. Pharm. Biopharm. 109 (2016) 158–164, https://doi.org/10.1016/j.ejpb.2016.10.004.

[15] Á. Aguilar-de-Leyva, T. Sharkawi, B. Bataille, G. Baylac, I. Caraballo, Release behaviour of clozapine matrix pellets based on percolation theory, Int. J. Pharm. 404 (2011) 133–141.

[16] M.D. Campiñez, C. Ferris, M. V de Paz, A. Aguilar-de-leyva, J. Galbis, I. Caraballo, A new biodegradable polythiourethane as controlled release matrix polymer, Int. J. Pharm. 480 (2015) 63–72, https://doi.org/10.1016/j.ijpharm.2015.01.011.

[17] I. Caraballo, M. Fernández-Arévalo, M. Millán, A.M. Rabasco, H. Leuenberger, Study of percolation thresholds in ternary tablets, Int. J. Pharm. 139 (1996) 177–186.

[18] Á. Aguilar-De-Leyva, C. Cifuentes, A.R. Rajabi-Siahboomi, I. Caraballo, Study of the critical points and the role of the pores and viscosity in carbamazepine hydrophilic matrix tablets, Eur. J. Pharm. Biopharm. 80 (2012) 136–142, https://doi.org/10.1016/j.ejpb.2011.09.007.

[19] Á. Aguilar-de-Leyva, M.D. Campiñez, F. Jost, M. Gavira, I. Caraballo, Study of the critical points in combined matrix tablets containing both inert and swelling excipients, J. Drug Deliv. Sci. Technol. 52 (2019) 885–894, https://doi.org/10.1016/j.jddst.2019.06.005.

[20] L. Contreras, L.M. Melgoza, R. Villalobos, I. Caraballo, Study of the critical points of experimental HPMC-NaCMC hydrophilic matrices, Int. J. Pharm. 386 (2010) 52–60, https://doi.org/10.1016/j.ijpharm.2009.10.048.

[21] A. Miranda, M. Millán, I. Caraballo, Study of the critical points of HPMC hydrophilic matrices for controlled drug delivery, Int. J. Pharm. 311 (2006) 75–81, https://doi.org/10.1016/j.ijpharm.2005.12.012.

[22] I. Caraballo, M. Fernandez-Arevalo, M.A. Holgado, A.M. Rabasco, H. Leuenberger, Study of the release mechanism of carteolol inert matrix tablets on the basis of percolation theory, Int. J. Pharm. 109 (1994) 229–236.

[23] L.M. Mason, M.D. Campiñez, S.R. Pygall, J.C. Burley, P. Gupta, D.E. Storey, I. Caraballo, C.D. Melia, The influence of polymer content on early gel-layer formation in HPMC matrices: the use of CLSM visualisation to identify the percolation threshold, Eur. J. Pharm. Biopharm. 94 (2015) 485–492, https://doi.org/10.1016/j.ejpb.2015.06.019.

[24] M. Casas, E. Galdón, D.J. Ojeda, I. Caraballo, Thermoplastic polyurethane as matrix forming excipient using direct and ultrasound-assisted compression, Eur. J. Pharm. Sci. (2019), https://doi.org/10.1016/j.ejps.2019.06.003.

[25] M. Casas, Á. Aguilar-de-Leyva, I. Caraballo, Towards a rational basis for selection of excipients: excipient Efficiency for controlled release, Int. J. Pharm. 494 (2015) 288–295, https://doi.org/10.1016/j.ijpharm.2015.08.002.

[26] I. Caraballo, M. Millán, A.M. Rabasco, H. Leuenberger, Zero-order release periods in inert matrices. Influence of the distance to the percolation threshold, Pharm. Acta Helv. 71 (1996) 335–339, https://doi.org/10.1016/S0031-6865(96)00023-4.

[27] T. Gonçalves-Araújo, A.R. Rajabi-Siahboomi, I. Caraballo, Application of percolation theory in the study of an extended release Verapamil hydrochloride formulation, Int. J. Pharm. 361 (2008) 112–117, https://doi.org/10.1016/j.ijpharm.2008.05.022.

[28] I. Caraballo, L. Melgoza, J. Alvarez-Fuentes, M. Soriano, A. Rabasco, Design of controlled release inert matrices of naltrexone hydrochloride based on percolation concepts, Int. J. Pharm. 181 (1999) 23–30, https://doi.org/10.1016/S0378-5173(98)00415-3.

[29] I. Caraballo, M. Millán, A. Fini, L. Rodriguez, C. Cavallari, Percolation thresholds in ultrasound compacted tablets, J. Contr. Release 69 (2000) 345–355.

[30] N. Ramírez, L.M. Melgoza, M. Kuentz, H. Sandoval, I. Caraballo, Comparison of different mathematical models for the tensile strength-relative density profiles of binary tablets, Eur. J. Pharm. Sci. 22 (2004) 19–23, https://doi.org/10.1016/j.ejps.2004.02.002.

[31] Á. Aguilar-de-Leyva, M.D. Campiñez, M. Casas, I. Caraballo, Design space and critical points in solid dosage forms, J. Drug Deliv. Sci. Technol. 42 (2017) 134–143, https://doi.org/10.1016/j.jddst.2017.06.004.

[32] C.G. Dillon, P.F. Carey, R.H. Worden, Fractscript: a macro for calculating the fractal dimension of object perimeters in images of multiple objects, Comput. Geosci. 27 (2001) 787–794, https://doi.org/10.1016/S0098-3004(00)00171-0.

[33] T. Higuchi, Mechanism of sustained-action medication. Theoretical analysis of rate of release of solid drugs dispersed in solid matrices, J. Pharmacol. Sci. 52 (1963) 1145–1149.

[34] R.W. Korsmeyer, R. Gurny, E. Doelker, P. Buri, N.A. Peppas, Mechanisms of solute release from porous hydrophilic polymers, Int J Pharm 15 (1983) 25–35.

[35] P.L. Ritger, N.A. Peppas, A simple equation for description of solute release I. Fickian and non-fickian release from non-swellable devices in the form of slabs, spheres, cylinders or discs, J. Contr. Release 5 (1987) 23–36.

[36] J.D. Bonny, H. Leuenberger, Matrix type controlled release systems: I. Effect of percolation on drug dissolution kinetics, Pharm. Acta Helv. 66 (1991) 160–164.

[37] A. Boza, R. Blanquero, M. Millan, I. Caraballo, Application of a new mathematical method for the estimation of the mean surface area to calculate the percolation threshold of lobenzarit disodium salt in controlled release matrices, Chem. Pharm. Bull. 52 (2004) 797–801, https://doi.org/10.1248/cpb.52.797.

[38] H. Fessi, J.P. Marty, F. Puisieux, J.T. Carstensen, The Higuchi square root equation applied to matrices with high content of soluble drug substance, Int. J. Pharm. 1 (1978) 265–274, https://doi.org/10.1016/0378-5173(78)90024-8.

[39] M. Millán-Jiménez, E. Galdón, C. Ferrero, I. Caraballo, Application of ultrasound-assisted compression in pharmaceutical technology . Design and optimization of oral sustained-release dosage forms, J. Drug Deliv. Sci. Technol. 42 (2017) 119–125.

[40] I. Fuertes, A. Miranda, M. Millán, I. Caraballo, Estimation of the percolation thresholds in acyclovir hydrophilic matrix tablets, Eur. J. Pharm. Biopharm. 64 (2006) 336–342, https://doi.org/10.1016/j.ejpb.2006.05.009.

[41] H. Leuenberger, Application of percolation theory in powder technology, Adv. Powder Technol. 10 (1999) 323–352, https://doi.org/10.1163/156855299X00190.

[42] L.E. Holman, H. Leuenberger, The effect of varying the composition of binary powder mixtures and compacts on their properties: a percolation phenomenon, Powder Technol. 60 (1990) 249–258, https://doi.org/10.1016/0032-5910(90)80124-H.